Journal of The Electrochemical Society, **159** (5) B483-B488 (2012)
0013-4651/2012/159(5)/B483/6/$28.00 © The Electrochemical Society

Nitrogen- and Boron-Doped Carbon Nanotube Electrodes in a Thermo-Electrochemical Cell

Pablo F. Salazar,[a] Satish Kumar,[a] and Baratunde A. Cola[a,b,z]

[a]*George W. Woodruff School of Mechanical Engineering and* [b]*School of Materials Science and Engineering, Georgia Institute of Technology, Atlanta, Georgia 30332, USA*

We explore the prospects of using doped carbon nanotube (CNT) electrodes to increase the output power of thermo-electrochemical cells (TECs). CNT buckypaper electrodes doped with nitrogen and boron were characterized using cyclic voltammetry, impedance spectroscopy, and TEC test with potassium ferri/ferrocyanide electrolyte. Both doping states increased the electrochemically active surface area of CNT electrodes. Electrostatic interactions with potassium ions altered the charge transfer kinetics for doped CNT electrodes; yet, the symmetry of the charge transfer remained approximately equal to that of pristine CNTs. In TEC test, accumulation of potassium ions at doped CNT electrodes was found to reduce short-circuit current.
 [DOI: 10.1149/2.043205jes]

Manuscript submitted December 23, 2011; revised manuscript received February 2, 2012. Published February 28, 2012.

Increased global consumption of energy compels us to discover and develop efficient, cost-effective, and durable sustainable energy converters. Recent studies demonstrated that thermo-electrochemical cells (TECs) with carbon nanotubes (CNTs) as electrodes,[1] or with non-aqueous solutions,[2–5] could develop into a viable sustainable energy source because of their potential low cost, maintenance-free, environmentally benign operation, and mechanical flexibility with potential heat sources. TECs are electrochemical analogs to thermoelectric devices.[6–11] Redox reactions at electrodes and ionic conductivity in the bulk substitute for the electronic conduction in solid-state thermoelectric devices, and the thermal dependence of the electrode potential is the driving source of voltage generation instead of the Seebeck effect.

TECs, also known as thermogalvanic cells or thermocells, operate under a thermal gradient established by heat flow through the cell. The voltage and current generated in TECs are proportional to the reaction entropy and charge transfer rate constant of the redox couple, respectively. The open circuit potential can be expressed as

$$V_{oc} = \frac{S_{rx}\Delta T}{nF}, \qquad [1]$$

where S_{rx} is the reaction entropy of the redox reaction $R \leftrightarrow O + ne^-$, F is the Faraday constant, and ΔT is the temperature difference between the cold and hot electrode.

At operational conditions, the current in a TEC is determined by the ohmic charge transfer (Butler-Volmer relationship), diffusion (Fick's law), and thermal diffusion (Soret effect) resistances, and can be expressed as:

$$I = {}^{V}/_{(R_{charge\ transfer} + R_{diffusion} + R_{ohmic} + R_{thermal\ dif.})}. \qquad [2]$$

To maximize net power, redox couples with high exchange current densities and reaction entropies such as ferri/ferrocyanide are usually employed in TECs.[1,12,13]

In TECs, as in any electrochemical device, catalytic electrodes with high exchange current densities are one of the major limitations in energy conversion. In addition to the high accessible surface area of CNT electrodes, their catalytic activity toward oxidation and reduction reactions has found application in several electrochemical devices (e.g., batteries, sensing, fuel cells, and TECs).[1,14–18] In particular, the fast kinetics of CNTs with ferri/ferrocyanide has been reported by Nugent et al.[12] Another attractive characteristic of CNTs is the relative ease of functionalizing or doping them[19] to potentially alter their properties. For example, nitrogen doped CNTs have been shown to have a greater electrocatalytic activity than pristine CNTs toward oxygen reduction reactions.[20] Boron-doped CNTs have been reported to enhance electron field emission[21] and improve electrochemical detection of NADH and L-cysteine.[22,23] Additional studies of the kinetics of doped CNT electrodes and demonstrations of their use in other applications are difficult to find in the literature. Furthermore, as pointed out by Quickenden et al. in his review of TECs,[13] open circuit, voltages and current densities using p- and n-type electrodes have, surprisingly, not been explored.

Here, we investigate nitrogen-doped CNT (NCNT) and boron-doped CNT (BCNT) electrodes in order to improve the catalytic activity of CNT electrodes with the ferri/ferrocyanide redox couple, and to potentially improve the energy conversion efficiency of CNT-based TECs. Cyclic voltammetry (CV) measurements revealed a reversible (i.e., diffusion controlled) electrochemical reaction at NCNT electrodes at low electrolyte concentrations and a more irreversible reaction at high concentrations, suggesting slower kinetics at higher electrolyte concentrations. In contrast, slow kinetics was observed for BCNT electrodes at both low and high electrolyte concentrations. CV results for both NCNT and BCNT electrodes suggest that plasma exposure during the doping process increased the electrochemically active surface area. An apparent change of the symmetry of the charge transfer coefficient with NCNT and BCNT electrodes was not reflected in CV scans.

Experimental Details

Electrode preparation and doping.— Multiwall CNT buckypaper was purchased from Nanocomp, Inc. The multiwall CNT buckypaper (Fig. 1A) is approximately 35 μm thick, with CNT lengths ∼100 μm and diameters approximately 10 nm. The content of doping element in the CNTs was controlled to approximately 5% with respect to carbon using a plasma-enhanced chemical vapor deposition (PECVD) process. Nitrogen doping of buckypaper samples was obtained after 5 minutes exposure to 350 W RF plasma (13.56 MHz) and 250 sccm of nitrogen (N_2) mixed with 20 sccm of ammonia (NH_3); the process chamber was at 200 mTorr and 350°C. Boron doping followed a similar process with a mixture of silane (SiH_4) and diborane gas (B_2H_6) at 300 mTorr replacing N_2 and NH_3 in the process chamber. Figure 1B shows X-ray photoelectron spectroscopy (XPS) data for NCNT and BCNT electrodes with peaks at the corresponding energy level of the dopant element (195 eV for boron and 400 eV for nitrogen). Platinum (Pt) electrodes were fabricated for comparison with CNT electrodes by sputtering a 50/150 nm bilayer of Ti/Pt on a stainless steel substrate. The geometric surface area of all electrodes was held constant at 0.178 cm.[2]

Characterization methods.— Cyclic voltammetry (CV) and impedance spectroscopy (EIS) measurements were carried on a CH660D potentiostat. Ohmic resistance compensation was applied

[z] E-mail: cola@gatech.edu

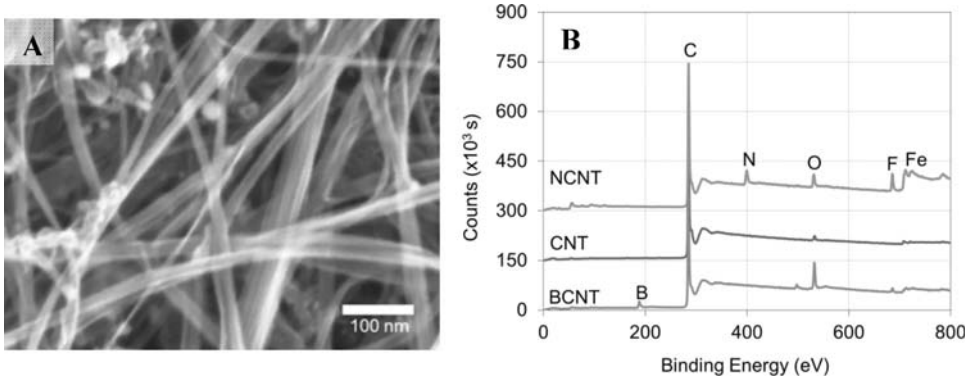

Figure 1. (A) Scanning electron microscope (SEM) micrograph of MWNT buckypaper. (B) X-ray photospectroscopy (XPS) of buckypaper before and after nitrogen and boron doping.

to all CV runs. EIS data was taken at the equilibrium potential dc signal (with respect to Ag/AgCl reference electrode) and 5 mV amplitude ac signal. The electrolyte solution was potassium ferrocyanide and potassium ferricyanide (Sigma-Aldrich) dissolved in distilled water. Both measurements, EIS and CV, were performed at several times after immersion of the electrodes in the electrolyte solution and the final measurements reported do not change significantly with time. EIS and CV runs were performed at 20°C.

Results and Discussion

Electrochemical characterization.— The diameter of the semicircle in the frequency range of kinetic control determines the charge transfer resistance in EIS according to the Randles model.[24] The charge transfer resistances of Pt and CNT electrodes were estimated from their EIS responses in 0.01 M of ferri/ferrocyanide solution (Fig. 2) to be 23 Ω and 92 Ω, respectively. The diffusion and kinetic controlled EIS responses superpose for doped CNT electrodes because of their large capacitances; therefore, it is difficult to estimate charge transfer resistance for doped CNTs using EIS. The ohmic resistances due to the electrodes, solution, and interfaces were determined by extrapolating measurements at high frequencies (left side of the curve) using the Randles model. As expected, injection of electrons (NCNT) and holes (BCNT) increase and decrease the electronic conductivity of CNT electrodes, respectively.

Electrodes of NCNTs, pristine CNTs, and Pt produce a separation of about 60 mV between peak potentials in 0.01 M of potassium ferri/ferrocyanide at a CV scan rate of 10 mV/s and 20°C (Fig. 3); this corresponds to a reversible electrochemical reaction. In contrast, BCNT electrodes produce a peak separation of 250 mV, which indicates sluggish charge transfer (i.e., quasi-reversible kinetics).

The reduction and oxidation at the surface is fast enough to maintain dynamic equilibrium of the anodic and cathodic current at any voltage in reversible electron transfer kinetics. The maximum current occurs when the reactant ion concentration at the electrode surface is dominated by mass diffusion. The peak current at the electrode is

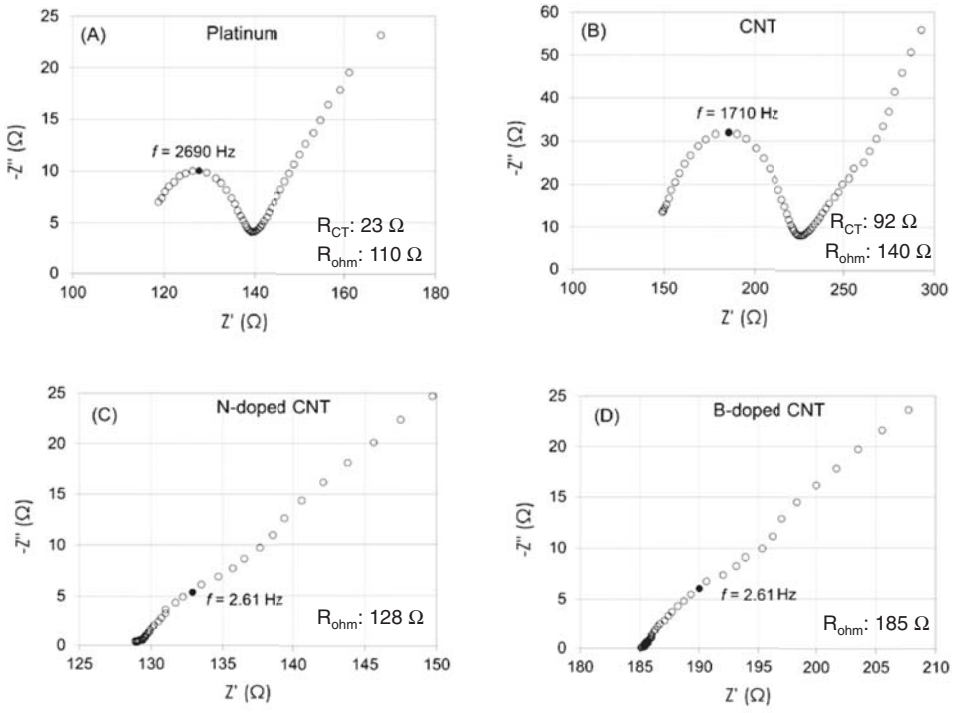

Figure 2. Electrochemical impedance spectroscopy (EIS) at 190 mV dc signal, 5 mV ac signal, and 0.01 M equimolar solution of $K_3Fe(CN)_6/K_4Fe(CN)_6$. R_{CT}: charge transfer resistance. R_{ohm}: ohmic resistance.

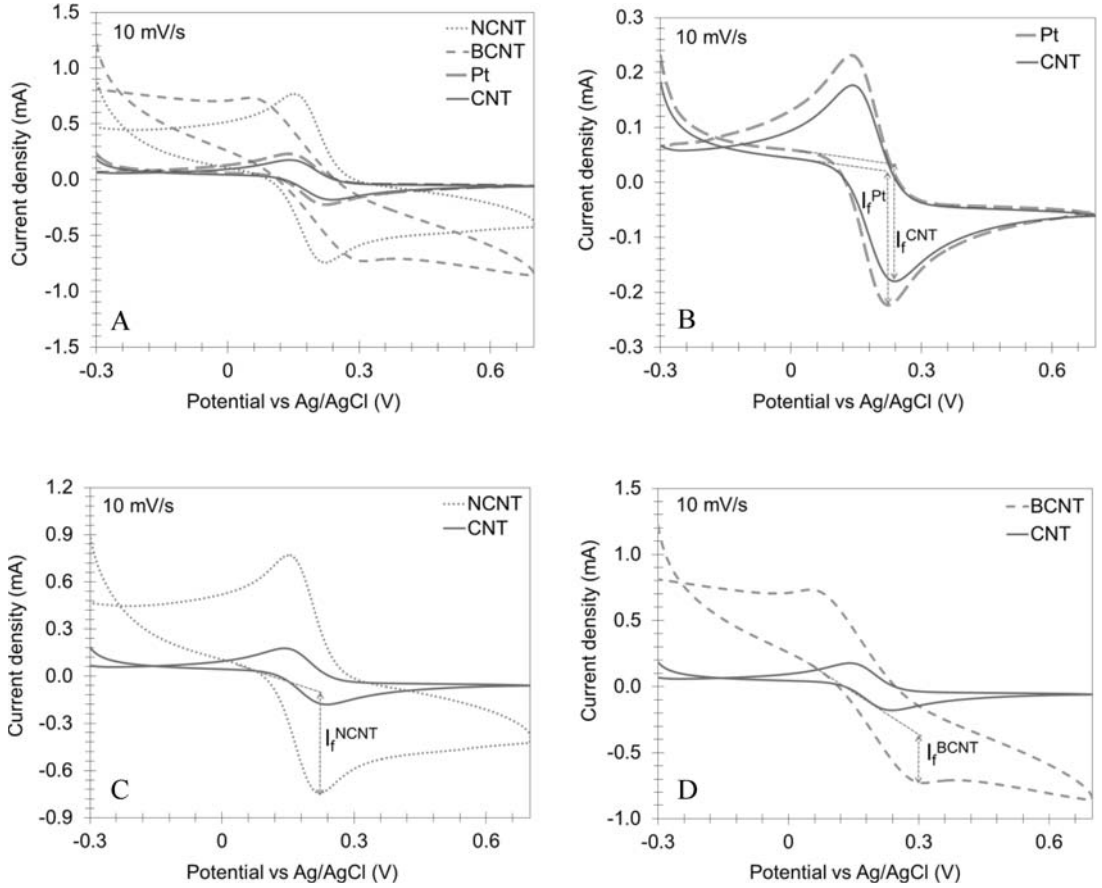

Figure 3. Cyclic voltammetry of 0.01 M equimolar solution of $K_3Fe(CN)_6/K_4Fe(CN)_6$ at 10 mV/s and 20°C. Voltage scan starts at −0.3 V (with respect to a Ag/AgCl reference electrode). IR compensation was applied before every run. Geometric surface area is 0.178 cm^2.

independent of the exchange current density constant (i.e., the dynamic equilibrium current at zero voltage) as well as the potential where the peak current occurs. The faradaic peak current (I_{p_f}) varies proportionally to the diffusion coefficient (D), initial concentration (c_o), scan rate (ν), and electroactive surface area (A) as described in[25]

$$I_{p\_f} \propto \sqrt{D\nu}c_o A. \quad [3]$$

Cyclic voltammetry experiments on all of the electrodes indicate purely capacitive current from −0.3 V (V_i) to 0 V (V_f). The average capacitance (γ) can be estimated by integrating the current within this voltage window as described in

$$\gamma = \frac{1}{\nu(V_f - V_i)} \int_{V_i}^{V_f} I(V)dV. \quad [4]$$

The specific capacitances of NCNT and BCNT electrodes (with respect to the geometric surface area) are 180 mF/cm^2 and 316 mF/cm^2, respectively (Fig. 3C and 3D); the capacitance of pristine CNT electrodes is 42 mF/cm^2 at the same concentration and scan rate. Because NCNT and CNT electrodes both have reversible kinetics, the increase in the peak faradaic current for NCNT (0.71 mA compared to 0.23 mA for CNT) can only result from a change in the effective electroactive surface area (according to Eq. 3). This hypothesis is supported by the similar 3- to 4-fold increase in capacitance and faradaic current of NCNT with respect to pristine CNT electrodes. The peak faradaic current of BCNT electrodes (0.36 mA) is greater than that of CNT electrodes because of the increase in surface area; however it does not show a 3-fold increase, as is the case with NCNT electrodes, because of the irreversibile charge transfer kinetics (Fig. 3). We attribute the increase in surface area of doped electrodes to structural changes that likely result from the breaking of C-C bonds and dopant substitution during the PECVD doping process.

When the voltage sweep rate in CV is increased, the reactions of ions at the surface are not able to maintain equilibrium with the potential of the electrode. The system presents quasi-reversible kinetics at this state, and thus the peak currents and peak potentials will depend on the electrochemical kinetics as well as mass transfer properties. The kinetics can be analyzed qualitatively using the separation of the potential peaks where slow kinetics will need more voltage or time to reach the peak current or the current where depletion of ions at the surface commences. The CV in Fig. 4B shows that the separation between peak potentials is 40 mV smaller for NCNT electrodes than it is for CNT electrodes at a scan rate of 100 mV/s in 0.01 M ferri/ferrocyanide solution. This shows that nitrogen doping improves the kinetics of CNT electrodes. Boron doped CNT electrodes show much slower kinetics than both NCNT and CNT electrodes, which is consistent with results from scans at 10 mV/s. A possible explanation of the changes in electrode kinetics with doping is associated with electrostatic effects at the electrode-electrolyte interface, which alter the electrochemical double layer as well as the interactions with counterions. Although still unclear, the effect of non-covalent interactions between ions and the electrode have been shown to be important in the kinetics.[26] According to the Gouy-Chapman-Stern model,[27] electrostatic forces near the electrode cause an exponential distribution of the ion concentration as described by

$$c_{si} = c_{oi} \exp\left(\frac{z_i \phi F}{RT}\right). \quad [5]$$

The charge of the ion and its concentration at the surface and in the bulk are represented by z_i, c_{si} and c_{oi}, respectively. The potential

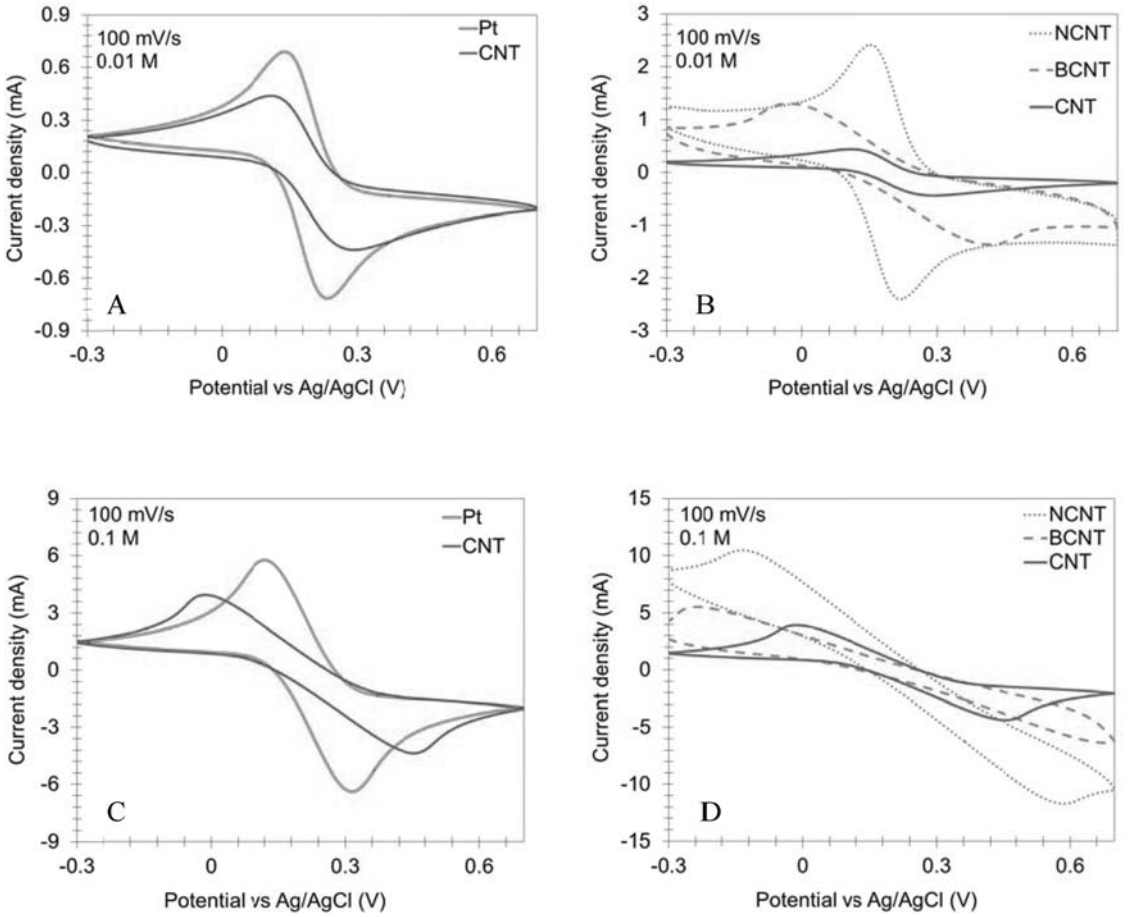

Figure 4. Cyclic voltammetry of 0.01 M (A and B) and 0.1 M (C and D) equimolar solution of $K_3Fe(CN)_6/K_4Fe(CN)_6$ at 100 mV/s and 20°C. Voltage scan starts at −0.3 V (with respect to a Ag/AgCl reference electrode). IR compensation was applied before every run. Geometric surface area is 0.178 cm^2.

at the surface of the electrode with respect to the potential at the bulk is ϕ. According to Eq. 5, a negatively charged doped electrode (NCNT) strengthens the electrostatic interaction with potassium (K+) counter ions and increases the electrolyte concentration at the surface of the electrode; the net current increases as a result. Similarly, a positively charged doped electrode will repulse the K+ and reduce the net current.

Because anodic and cathodic peak currents are a function of the exchange current density constant in quasi-reversible reactions,[25] they are also a function of the charge transfer coefficient, which describes the preference of the charge transfer to either reduction or oxidation reactions. The charge transfer coefficients toward oxidation and reduction may be different, but their sum equals 1. Although the doping seems to alter the fermi energy of the electrodes and therefore the energy gap with respect to the electrolyte – as indicated by the change in electrode resistance with doping shown in Fig. 2; Fig. 4 shows that the relative distance of anodic (Epa) and cathodic (Epc) peak potential with respect to the equilibrium potential (Eeq) is the same in irreversible CV plots for any electrode ($|E_{pa}-E_{eq}| = |E_{pc}-E_{eq}|$). This therefore suggests that the anodic and cathodic charge transfer coefficients are close to 0.5 with NCNT and BCNT electrodes in potassium ferri/ferrocyanide electrolyte (since the sum has to be equal to 1).[25] When the charge transfer coefficient is symmetric, the electrodes interact identically with oxidized and reduced metal ions. Also, the reactions can be considered adiabatic because doping CNT electrodes, and the resulting changes in electrical resistance, did not appear to alter the transfer coefficients. Therefore, changes to electrode kinetics with doped CNT electrodes (see Fig. 4) probably result only from changes to the frequency of redox ion collisions with the electrodes and the associated activation energies for these processes.

Cyclic voltammetry scans at 100 mV/s were also performed at a higher electrolyte concentration of 0.1 M potassium ferri/ferrocyanide (Fig. 4C and 4D) because such high concentrations are required for practical TECs. The separation of potential peaks for Pt, CNT and BCNT electrodes shows slower kinetics for BCNTs than that of CNTs, and slower kinetics for CNTs than that of Pt. These trends are similar to the trends observed at lower concentrations. However, in contrast to results at low electrolyte concentration, NCNT electrodes show slower

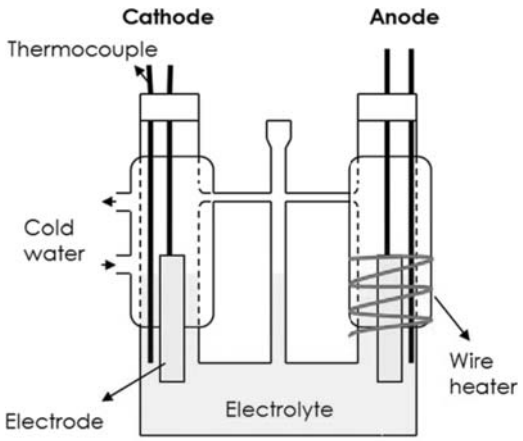

Figure 5. Schematic representation of the U-cell configuration for thermocell testing.

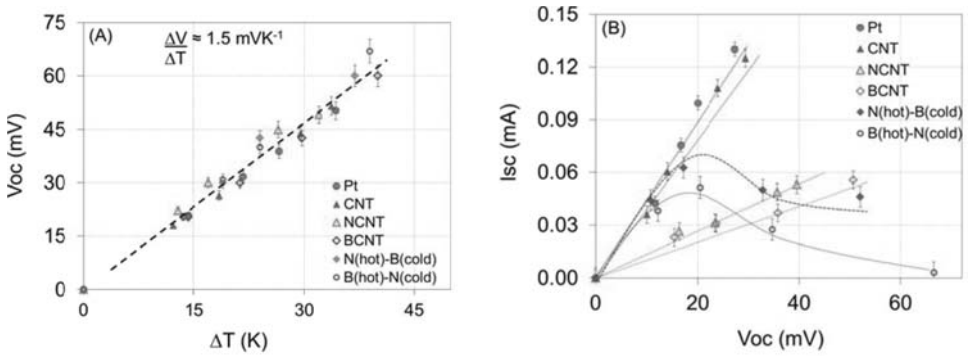

Figure 6. TEC response in 0.1 M equimolar solution of $K_3Fe(CN)_6/K_4Fe(CN)_6$. A: Open-circuit potential (V_{oc}) and B: short-circuit current (I_{sc}). Temperature at the cold electrode was maintained at 20°C. Geometric surface area is 0.178 cm^2. Ohmic resistance compensation was applied to the short circuit current reported. The same electrode type was used as the anode and cathode unless otherwise stated in the legend.

kinetics than that of CNT and Pt electrodes at the higher concentration; the redox reactions at NCNT electrodes are no longer reversible at high concentrations. In this case, high bulk concentrations decrease the thickness of the electrochemical double layer[27] in the order of $[10^7|z_i|(c_i^o)^{0.5}]^{-1}$; this adds to the compression of the double layer that already exists due to the negatively charged doped electrode (NCNT). We expect that the high density of electrolyte (especially K+) blocks the path to oxidation and reduction for metal ions at the electrode surface and slows down the kinetics as a result.

TEC performance.— The energy conversion efficiency of a TEC is approximated as

$$\eta = \frac{V_{oc} I_{sc}}{4A\kappa\Delta T/d}, \qquad [6]$$

where V_{oc} is the open circuit voltage, I_{sc} the short circuit current, A the geometric surface area, κ the thermal conductivity of the electrolyte, ΔT the temperature difference and d the distance between electrodes. Here, we measure V_{oc} and I_{sc} for Pt, CNT, and doped CNT electrodes in the same U-cell configuration (Fig. 5); the results are presented in Fig. 6. The open circuit potential is driven by a thermal gradient (as described in Eq. 1) and the ratio $V_{oc}/\Delta T$ is approximately 1.5 mV/K for all electrodes (see Fig. 6A). The short-circuit currents at steady state correlate with trends in the charge transfer kinetics shown in the CV scans at high electrolyte concentration of Fig. 4C and 4D (these scans were performed in the same electrolyte concentration used for TEC tests). The lower I_{sc} for NCNT and BCNT electrodes compared to that of CNT and Pt electrodes (Fig. 6B) reflects their relatively sluggish charge transfer kinetics as discussed above. Balanced kinetic rates exist in symmetric NCNT and BCNT electrode configurations so that the current increases linearly with potential as it does for symmetric CNT and Pt electrode configurations. The performance of asymmetric doped electrode configurations is also shown in Fig. 6, i.e., NCNT as the cold electrode and BCNT as the hot electrode, and vice versa. While both asymmetric arrangements produce higher initial currents than symmetric doped electrode configurations, the current in the asymmetric arrangements eventually decreases as the magnitude of the thermal gradient is increased. The combination of BCNT and NCNT electrodes at small thermal gradients drives large concentration gradients at the surface of the BCNT electrode due to its slow kinetics while establishing low surface concentrations at the NCNT electrode, which avoids the blocking state discussed in the previous section. At larger thermal gradients, the ion concentration at the surface of NCNT electrodes increases to the point where the high collision of ions slows the kinetics and reduces the currents. The electrostatically altered kinetic rates are imbalanced with asymmetric electrodes so an accumulation of electrolyte concentration at the electrode with the slower kinetics is expected. This accumulation of concentration is likely the cause of the non-linear decrease in current with increased thermal gradient or potential in the asymmetric configurations. The transition to slower kinetics occurs at smaller thermal gradients when the NCNT electrode is the cold electrode as opposed to the hot electrode because higher ion concentrations exist at the cold electrode because of the relatively slow kinetics at low temperatures. The NCNT symmetric configuration shows lower currents than any of the asymmetric cases because the interfacial blocking state is reached in a similar way at the hot and cold electrodes.

Conclusions

In summary, the results of this study suggest that the process of doping CNT electrodes can change the electroactive surface area by as much as 3- to 4-fold. In addition, electrostatic interactions between counterions and the electrodes should be considered in the search for electrodes with improved electron transfer kinetics. Doped CNT electrodes did not exhibit an apparent change in the kinetic transfer coefficient with the ferri/ferrocyanide redox couple, which indicates that the reaction is adiabatic. Alternative counterions such as sodium or lithium, or electrodes with higher density of CNTs that are accessible to the electrolyte should be explored in order to utilize doped CNT electrodes to improve the performance of TGCs.

Acknowledgments

We are grateful for the financial support of National Science Foundation Awards No. CBET 1055479 and No. DMR 0120967 (through a seed grant), and support provided by the Georgia Institute of Technology Woodruff School of Mechanical Engineering. We thank Dr. Virendra Singh for this assistance with SEM and XPS analysis.

References

1. R. Hu, B. A. Cola, N. Haram, J. N. Barisci, S. Lee, S. Stoughton, G. Wallace, C. Too, M. Thomas, A. Gestos, M. E. d. Cruz, J. P. Ferraris, A. A. Zakhidov, and R. H. Baughman, *Nano Letters*, **10**(3), 838 (2010).
2. T. J. Abraham, D. R. MacFarlane, and J. M. Pringle, *Chemical Communications*, **47**(22), 6260 (2011).
3. M. Bonetti, S. Nakamae, M. Roger, and P. Guenoun, *Journal of Chemical Physics*, **134**(11), 114513 (2011).
4. Y. Ito and T. Nohira, *Electrochimica Acta*, **45**(15–16), 2611 (2000).
5. Y. V. Kuzminskii, V. A. Zasukha, and G. Y. Kuzminskaya, *Journal of Power Sources*, **52**(2), 231 (1994).
6. J. N. Agar, in *Advances in Electrochemistry and Electrochem. Eng.*, edited by P. Delay (Interscience, New York, 1963), vol. 3.
7. T. Ikeshoji and F. N. B. de Nahui, *Journal of Electroanalytical Chemistry*, **305**(1), 147 (1991).
8. J. Josserand, V. Devaud, G. Lagger, H. Jensen, and H. H. Girault, *Journal of Electroanalytical Chemistry*, **565**(1), 65 (2004).
9. T. I. Quickenden and C. F. Vernon, *Solar Energy*, **36**(1), 63 (1986).
10. A. V. Sokirko, *Electrochimica Acta*, **39**(4), 597 (1994).
11. H. J. Tyrrell, in *Diffusion and Heat Flow in Liquids* (Butterworths, London, 1961).

12. J. M. Nugent, K. S. V. Santhanam, A. Rubio, and P. M. Ajayan, *Nano Letters*, **1**(2), 87 (2001).
13. T. I. Quickenden and Y. Mua, *Journal of The Electrochemical Society*, **142**(11), 3985 (1995).
14. K. Gong, Y. Yan, M. Zhang, L. Su, S. Xiong, and L. Mao, *Analytical Sciences*, **21**(12), 1383 (2005).
15. B. J. Landi, M. J. Ganter, C. D. Cress, R. A. DiLeo, and R. P. Raffaelle, *Energy & Environmental Science*, **2**(6), 638 (2009).
16. R. L. McCreery, *Chemical Reviews*, **108**(7), 2646 (2008).
17. A. Merkoçi, M. Pumera, X. Llopis, B. Pérez, M. del Valle, and S. Alegret, *TrAC Trends in Analytical Chemistry*, **24**(9), 826 (2005).
18. C. Wang, M. Waje, X. Wang, J. M. Tang, R. C. Haddon, and Yan, *Nano Letters*, **4**(2), 345 (2003).
19. L. S. Panchakarla, A. Govindaraj, and C. N. R. Rao, *ACS Nano*, **1**(5), 494 (2007).
20. K. Gong, F. Du, Z. Xia, M. Durstock, and L. Dai, *Science*, **323**(5915), 760 (2009).
21. J. C. Charlier, M. Terrones, M. Baxendale, V. Meunier, T. Zacharia, N. L. Rupesinghe, W. K. Hsu, N. Grobert, H. Terrones, and G. A. J. Amaratunga, *Nano Letters*, **2**(11), 1191 (2002).
22. C. Deng, J. Chen, X. Chen, M. Wang, Z. Nie, and S. Yao, *Electrochimica Acta*, **54**(12), 3298 (2009).
23. C. Deng, J. Chen, X. Chen, C. Xiao, Z. Nie, and S. Yao, *Electrochemistry Communications*, **10**(6), 907 (2008).
24. J. E. B. Randles, *Discussions of the Faraday Society*, **1**, 11 (1947).
25. A. J. Bard, *Electrochemical methods : fundamentals and applications* 2ed. (John Wiley & Sons, Inc, 2001).
26. D. Strmcnik, K. Kodama, D. van der Vliet, J. Greeley, V. R. Stamenkovic, and N. M. Marković, *Nat. Chem.*, **1**(6), 466 (2009).
27. P. Delahay, *Double layer and electrode kinetics*. (John Wiley & Sons, Inc, 1965).